Langmuir

Article

pubs.acs.org/Langmuir

Online Rheological Investigation on Ion-Induced Micelle Transition for Amphiphilic Polystyrene-*block*-Poly(acrylic acid) Diblock Copolymer in Dilute Solution

Yuping Sheng,[†,‡] Nan Yan,[†] Yutian Zhu,*[,†] and Wei Jiang*[,†]

[†]State Key Laboratory of Polymer Physics and Chemistry, Changchun Institute of Applied Chemistry, Chinese Academy of Sciences, Changchun, Jilin 130022, People's Republic of China

[‡]College of Materials Science and Engineering, Jilin University, Changchun, Jilin 130022, People's Republic of China

Supporting Information

ABSTRACT: The ion-induced micellar transition is online-investigated by the time dependence of the viscosity of the solution under shear flow for the first time. During the morphological transition, the change in the micellar structure can be tracked by the change in viscosity. Adding HCl or $CaCl_2$ into pre-prepared spherical micelle solution from the self-assembly of polystyrene-*block*-poly(acrylic acid) (PS_{144}-*b*-PAA_{22}) in the *N*,*N*-dimethylformamide (DMF)/water mixture, the micellar structures change into short cylinders, long, entangled cylinders, and then lamellae or vesicles, corresponding to the viscosity increasing first and then declining. When HCl or $CaCl_2$ is added to the pre-prepared spherical micelle solution formed by PS_{144}-*b*-PAA_{50} in the dioxane/water mixture, the micellar structures are quickly transformed into cylinders or lamellae before carrying out the rheological measurement and then are turned to vesicles or spheres under the shearing, corresponding to a gradual decline in viscosity. This study shows that the rheology can be a very simple and effective online method on the investigation of the micellization, which plays an important role in understanding the micellization mechanism and micellar transition pathway of block copolymers in dilute solution.

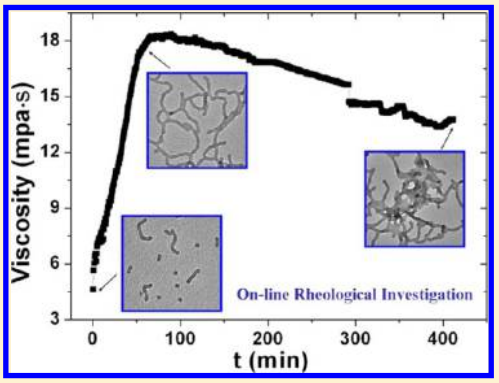

1. INTRODUCTION

The self-assembly of amphiphilic block copolymers in selective solution into various nanoscale micelles has received intensive attention in the last few decades, because of not only scientific interest but also their great potential applications, such as drug delivery,[1−4] separate,[5,6] and microreactors.[7] In general, the self-assembled morphologies include spheres,[8] cylinders,[8,9] rings,[10,11] and vesicles.[8,12,13] Besides exploring new micellar structures, the transitions between different micellar structures have also received widespread attention. For instance, it was observed that spheres can transform to cylinders and then to vesicles,[13−16] and the reversed transition process can also be achieved by changing the temperature.[17] Moreover, the ring-shaped micelles can be changed from cylinders or vesicles by tuning shear flow.[18]

To understand the micelle transitions, transmission electron microscopy (TEM) or scanning electron microscopy (SEM) was usually used to offline monitor the transition process. However, it is hard to precisely capture the intermediates in the micelle transition because of the limitation of the offline techniques. In addition to the offline techniques, there are also a few online techniques for the micelle transition, such as the small-angle neutron scattering (SANS) technique or rheo-nuclear magnetic resonance (NMR) technique. For instance, SANS was used to study the transition from vesicles to wormlike micelles.[19] The rheo-NMR was applied to online investigate the structural transition of aqueous solutions of regenerated silk fibroin by the time dependence of a series of ^{1}H NMR spectra under the shear flow.[20] On the other hand, it is known that the rheology is a widely used and sensitive online technique in polymer physics. Moreover, it has been proven that the rheological response of the micelle solution is highly relative to the micellar microstructure.[19,21−30] For example, Raghavan and co-workers reported that the vesicle−micelle transition caused the solutions to switch from low-viscosity, Newtonian fluids to viscoelastic, shear thinning fluids.[19] Shrestha et al. investigated the rheological behavior of viscoelastic wormlike micelles in mixed polyoxyethylene cholesteryl ethers and cocamide methyl monoethanolamine (MEA) aqueous systems.[27] They observed that the viscosity of the aqueous solution was increased by 5 orders of magnitude when the spherical micelles were transformed into rod-like micelles. Moreover, Morita et al. applied a rheological technique to study a heat-induced morphological transition from elongated micelles to flexible worm-like micelles.[31] This morphological transition caused a drastic increase in viscosity because of entanglement of the micelles. However, all of these

Received: April 22, 2014
Published: November 21, 2014

   dx.doi.org/10.1021/la503835u | *Langmuir* 2014, 30, 15392−15399

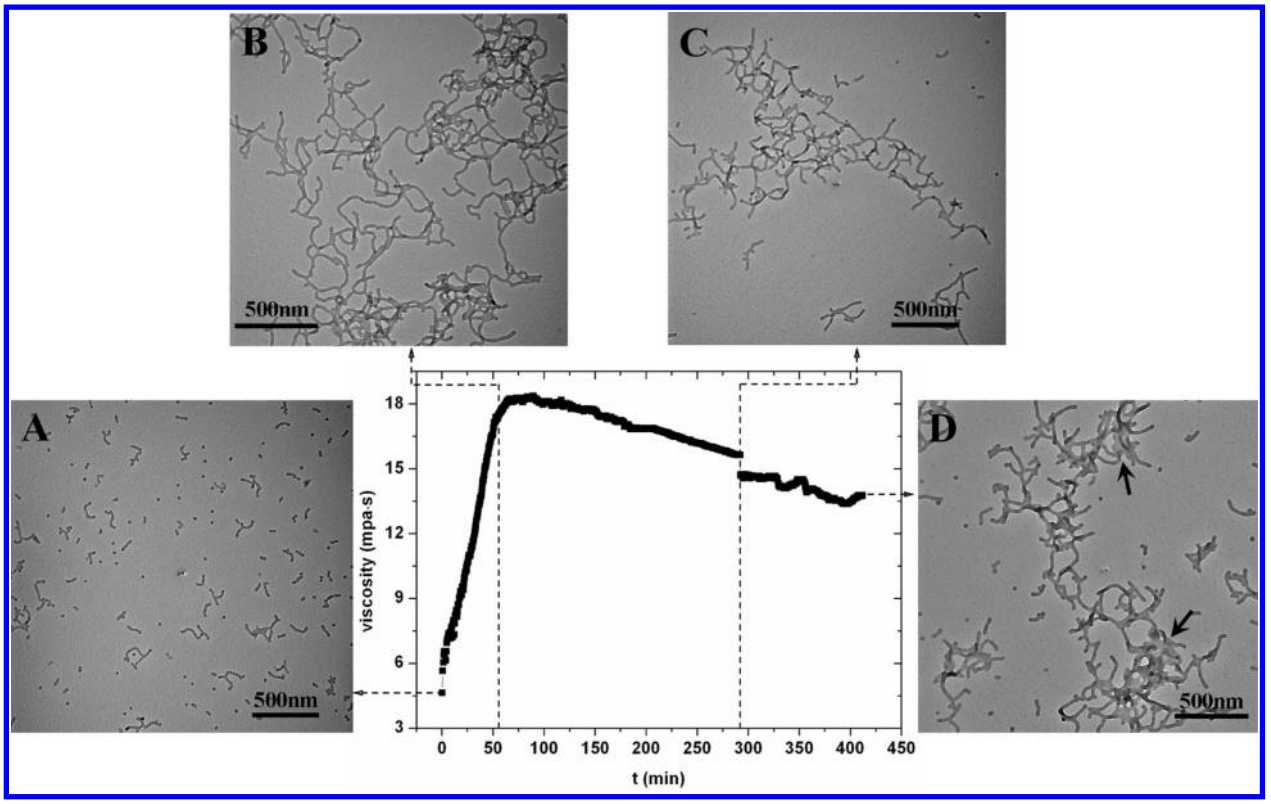

Figure 1. Viscosity as a function of the shear time after adding 30 μL (40 mmol/L) of HCl solution into the pre-prepared PS_{144}-*b*-PAA_{22} spherical micelle solution (500 μL) with interrupting the measurement to take a trace amount of micelle solution for TEM measurement. The shear rate is 75 s^{-1}. Several TEM images at different times are inserted in the curves to show the morphological transition pathway: snapshot A, 0 min; snapshot B, 55 min; snapshot C, 290 min; and snapshot D, 412 min.

previous rheological studies on the micelle transitions are still offline investigations, which only compare the rheological properties of different micelle solutions. Thus far, it is still lacking an online rheological study on the micellar transition. This is because the co-solvent used in the micellization of amphiphilic block copolymers is usually volatile. The evaporation of solvent during the measurement will also cause the change in the rheological signal, which makes one not be able to identify the change in the rheological signal arisen from the micelle transition or from the solvent evaporation. In the current study, we achieved the online investigation of ion-induced micellar transition for polystyrene-*block*-poly(acrylic acid) (PS-*b*-PAA) diblock copolymer in *N*,*N*-dimethylformamide (DMF)/water or dioxane/water mixture solution by a new type of rheometer, i.e., Brookfield LVDV-III Ultra programmable rheometer. Because all of the rheological measurements are employed in an airtight sample cup, the influence of the solvent evaporation on the rheological data can be effectively eliminated. By the time dependence of the viscosity of the PS−PAA solution under the shear flow, the ion-induced morphological transitions were online-traced. TEM images confirm the micellar morphologies in the transition, which agree well with the viscosity curves.

2. EXPERIMENTAL SECTION

2.1. Materials. The amphiphilic diblock copolymers, polystyrene-*block*-poly(acrylic acid) (PS_{144}-*b*-PAA_{22}, M_n = 15 000 g/mol for PS block and M_n = 1600 g/mol for PAA block, with M_w/M_n = 1.10; PS_{144}-*b*-PAA_{50}, M_n = 15 000 g/mol for PS block and M_n = 3600 g/mol for PAA block, with M_w/M_n = 1.20), were purchased from Polymer Source. DMF, dioxane, $CaCl_2$, and HCl (16 mol/L) were supplied by Beijing Chemical Works. $CaCl_2$ was dried in a vacuum drying oven before use. All of the materials were directly used after receiving without further purifying.

2.2. Preparation of the Micelles. For PS_{144}-*b*-PAA_{22}, the diblock copolymer was first dissolved in DMF (a co-solvent for both PS and PAA blocks) to make a copolymer solution containing 3 wt % block copolymer. The solution was kept stirring for 1 day to make the copolymers completely dissolve in the co-solvent. Then, a given volume of deionized water (6 wt % of the solution) was added (at the rate of 1 wt %/30 s) into the solution with stirring. After the water content reached 6 wt %, the solution was kept stirring at room temperature for 1 day to make the aggregates reach equilibrium. At this water content, the PS−PAA diblock copolymers tended to aggregate into spherical micelles. Then, the 30 μL of HCl solution or $CaCl_2$ solution was added to the sphere micelle solution (500 μL) to induce the micelle transition. After stirring for 20 s, 500 μL of solution was moved into the sample cup of the rheometer and then sheared at a certain rate for 7 h. For PS_{144}-*b*-PAA_{50} copolymer, ca. 2 wt % copolymer was dissolved in dioxane and the added deionized water was 9 wt %, with other steps being the same as the PS_{144}-*b*-PAA_{22} copolymer. When it is needed to take a sample from the sample cup for TEM measurement, the rheological measurement will be suspended. A trace amount of solution (3 μL) will be quickly taken from the sample cup to put into a large amount of (2 mL) methyl alcohol to quench the micellar structure for the TEM measurement. The micelle structures will then be kinetically locked because the micellar aggregates were isolated in methyl alcohol and the insoluble PS blocks were below their glass transition temperature after the quenching procedures.[8] It is also worth noting that such trace reduction of the solution will not affect the resume of rheological measurement.

2.3. Rheological Measurements. Rheological measurements were carried out on a Brookfield LVDV-III Ultra programmable rheometer at a given shear rate. The cone spindle used in the

dx.doi.org/10.1021/la503835u | *Langmuir* 2014, 30, 15392−15399

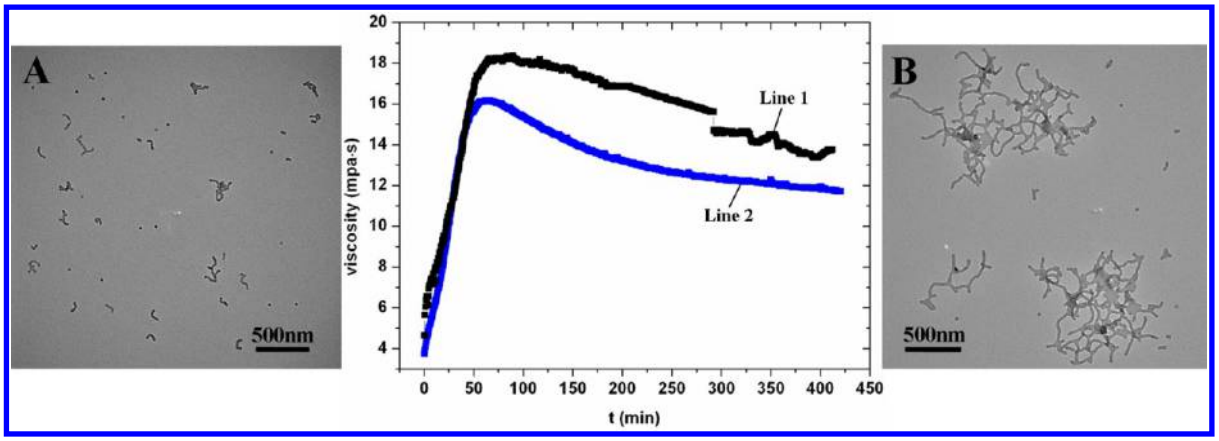

Figure 2. Viscosity as a function of the shear time after adding 30 μL (40 mmol/L) of HCl solution into the pre-prepared PS_{144}-*b*-PAA_{22} spherical micelle solution (500 μL) with interrupting the measurement to take a trace amount of micelle solution (line 1) and without interrupting the measurement (line 2). The shear rate is 75 s^{-1}. TEM images are for line 2: (A) t = 0 min and (B) t = 420 min.

measurement was CPE-40. The sample volume for the measurement was ca. 500 μL. The sample cup was airtight during the measurement, which could effectively prevent the solution evaporation. The shear rate was set at 75 s^{-1}, and the temperature was controlled at 20 °C.

2.4. TEM. The micellar morphologies during the micelle transition were visualized by the offline TEM. TEM measurements were performed on a JEOL JEM-1011 transition electron microscope operated at an acceleration voltage of 100 kV. A drop of the very dilute micellar solution was placed on the TEM grid (copper grids covered by a polymer support film precoated with carbon thin film) with a filter paper below to absorb the solution. The remaining micelle solution (methyl alcohol) on the grid was evaporated very fast at room temperature, while the micelles were deposited onto the grid surface for observation.

3. RESULTS AND DISCUSSION

The morphological transition of the supramolecular assemblies can generally be achieved by adding ions,[14,32−35] copolymers,[36−38] or surfactants[39−41] or changing the temperature.[17,42−44] In the current study, we add HCl or $CaCl_2$ into spherical micelle solution formed by PS_{144}-*b*-PAA_{22} in a DMF/water mixture or PS_{144}-*b*-PAA_{50} in a dioxane/water mixture to induce the morphological transition. The time dependence of the viscosity of the micelle solution under the shear flow was used to monitor the morphological transition that occurred in the solution. It is found that the change of viscosity can well reflect the morphological transition. When HCl or $CaCl_2$ is added to spherical micelle solution formed by PS_{144}-*b*-PAA_{22} in the DMF/water mixture, the micellar structures change into short cylinders, long and tangled cylinders, and then lamellae or vesicles, corresponding to a increase of viscosity at first and then a decrease of viscosity. When HCl or $CaCl_2$ is added to spherical micelle solution formed by PS_{144}-*b*-PAA_{50} in the dioxane/water mixture, the morphologies rapidly change into cylinder aggregates or lamellae before the rheological measurement and then into vesicles or spheres, corresponding to a gradual decrease in viscosity.

3.1. Online Rheological Investigation on the Morphological Transition Induced by HCl. PS_{144}-*b*-PAA_{22} diblock copolymers tend to form spherical micelles in the DMF/water mixture, which is confirmed by the TEM image, as shown in Figure S1a of the Supporting Information. After HCl solution is added, the introduced H^+ will hinder the ionization of PAA blocks, leading to the decrease of repulsive interactions of corona-forming chains, i.e., PAA chains.[33] The decrease of repulsive interactions of the PAA chains will cause the morphological transition. After 30 μL of HCl solution (40 mmol/L) is added to the spherical micelle solution (500 μL) and string for 20 s, the solution was removed into the rheometer sample cup to measure the viscosity under shear. The measured viscosity as a function of the shear time is presented in Figure 1. During the measurement, we took a trace amount of the micelle solution (3 μL) from the sample at times to do the TEM measurement for the visualization of the micellar structure. The obtained TEM images at different shear times are inserted in Figure 1 to show the morphological transition pathway. From the viscosity−time curve, it is observed that the viscosity of the micelle solution is increased at first and then declined. The TEM images show that the spheres have already transformed into short rods (snapshot A) at the beginning of the measurement (20 s after adding HCl solution). Then, these short rods transition into long and entangled cylinders (snapshot B) at 55 min. Because of the entanglement of flexible cylindrical micelles, we can observe a significant increase in the viscosity. Thereafter, long cylinders become shorter and shorter (snapshots C and D). The corresponding viscosity is then decreased because of the breakup of the entangled structures. Moreover, some cylinders start to merge into lamellae, as indicated by the arrows (snapshot D).

During the rheological measurement, a trace amount of micelle solution was taken from the sample cup. The trace reduction (3 μL) in the volume of the solution has negligible influence on the measurement result. Moreover, the solvent evaporation could also be negligible. This is because the operation for taking out the sample from the cup is controlled within 20 s, and the common solvents have relatively high boiling points (153 °C for DMF and 101 °C for dioxane) and low vapor pressures (2.6 mmHg at 20 °C for DMF and 4.1 mmHg at 20 °C for dioxane).[45] The slight fluctuations in the curve are mainly attributed to the temporary interruption of the shear flow. Once the shear is restarted, it needs some time to form uniform flow in the cone geometry again. To confirm the negligible influence of taking the sample on the measurement, we repeated the rheological measurement again. In the second measurement, there are no interruptions during the shearing. The viscosity−time curves for the first measurement (line 1, interrupted) and second measurement (line 2, not interrupted) are compared in Figure 2. These two curves are very similar,

dx.doi.org/10.1021/la503835u | *Langmuir* 2014, 30, 15392−15399

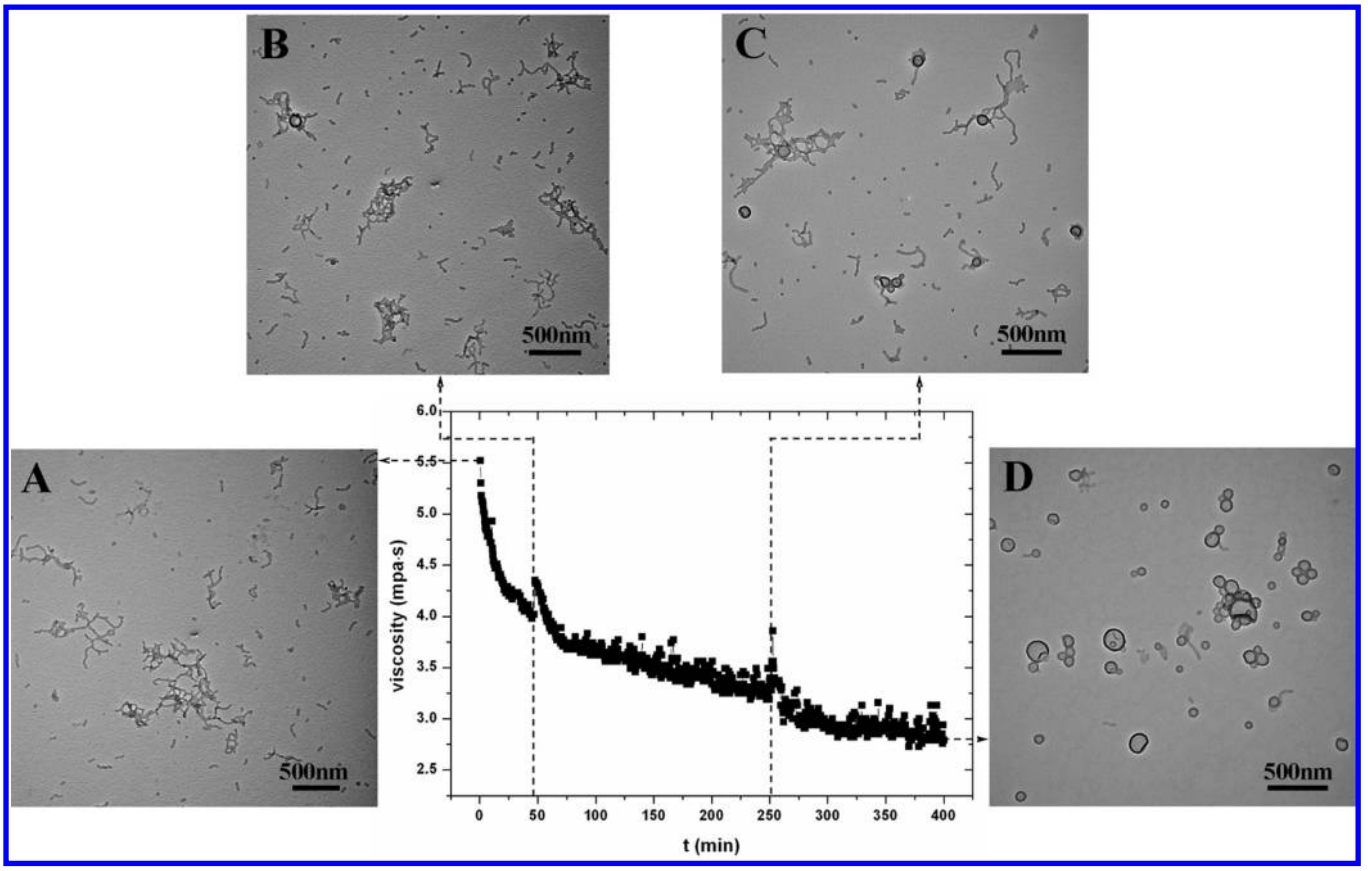

Figure 3. Viscosity as a function of the shear time after adding 30 μL (80 mmol/L) of HCl solution into the pre-prepared PS_{144}-*b*-PAA_{50} spherical micelle solution (500 μL). The shear rate is 75 s^{-1}. Several TEM images at different times are given to show the morphological transition pathway: snapshot A, 0 min; snapshot B, 47 min; snapshot C, 252 min; and snapshot D, 400 min.

which have a similar trend and peak value position. The initial morphology (before the rheological measurement) and the final morphology (after the rheological measurement) for the second measurement are shown in snapshots A and B of Figure 2, respectively. Clearly, these two morphologies also agree well with the snapshots A and D in Figure 1.

For another type of PS−PAA copolymer, i.e., PS_{144}-*b*-PAA_{50} copolymer, they also tend to form spherical micelles in a dioxane/water (1:0.09, v/v) mixture, as shown in Figure S1b of the Supporting Information. After 30 μL (80 mmol/L) of HCl solution is added into the pre-prepared PS_{144}-*b*-PAA_{50} spherical micelle solution (500 μL), the viscosity drops rapidly at first and then declines slowly with shear time, as shown in Figure 3. The viscosity−time curve indicates that the micellar structures are transformed from the entangled structures to the small separated structures. The TEM images at different shear times are also inserted in Figure 3 to show the morphological transition pathway. It is observed that the PS_{144}-*b*-PAA_{50} spheres have already transitioned into the entangled cylinders (snapshot A) at the beginning. Then, they become shorter and shorter (snapshot B), and then some lamellae and vesicles appeared (snapshot C). Finally, all of the lamellae are bent to form vesicles (snapshot D). Because the morphology transformed from long cylinders to small vesicles, there is a significant decrease of the viscosity, as shown in the viscosity−time curve shown in Figure 3. To prove that interrupting to take samples will also not affect the viscosity change and morphological transition, the viscosity curve obtained without interrupting and the corresponding TEM images of the morphologies before and after shear are shown in Figure S2 of the Supporting Information. To further confirm the morphological transition visualized by TEM, other visualization techniques, i.e., SEM and atomic force microscopy (AFM), are also used to visualize the micellar transitions shown in Figures 1 and 3. In Figures S3 and S4 of the Supporting Information, we compared the images from TEM, SEM, and AFM for the morphological transitions of PS_{144}-*b*-PAA_{22} and PS_{144}-*b*-PAA_{50} micelles, respectively. Clearly, the same micellar structures are observed by whatever visualization techniques.

In comparison of Figure 1 to Figure 3, it is found that the morphological transition pathways are different for PS_{144}-*b*-PAA_{22} and PS_{144}-*b*-PAA_{50}. The difference is mainly attributed to the different common solvents used for these two different types of copolymers. DMF is used for PS_{144}-*b*-PAA_{22}, while dioxane is used for PS_{144}-*b*-PAA_{50}. Eisenberg and co-workers proposed that the quality of the common solvent, i.e., the solubility parameters and dielectric constants of the solvent, plays a key effect on the PS-*b*-PAA micellar structure.[46] In that work, they found that the closer the match between the solubility parameter of the solvent and that of the core forming block, the higher the solvent content of the core and the higher the degree of stretching of the core chains. The lower the polarity of the solvent, the weaker the PAA−solvent interaction and the weaker the repulsive interactions among the corona chains. As the stretching degree of PS chains in the cores increases and the repulsion among the PAA corona decreases, the morphology of PS−PAA micelles changes from spheres to cylinders and then to vesicles or large compound micelles. In

dx.doi.org/10.1021/la503835u | *Langmuir* 2014, 30, 15392−15399

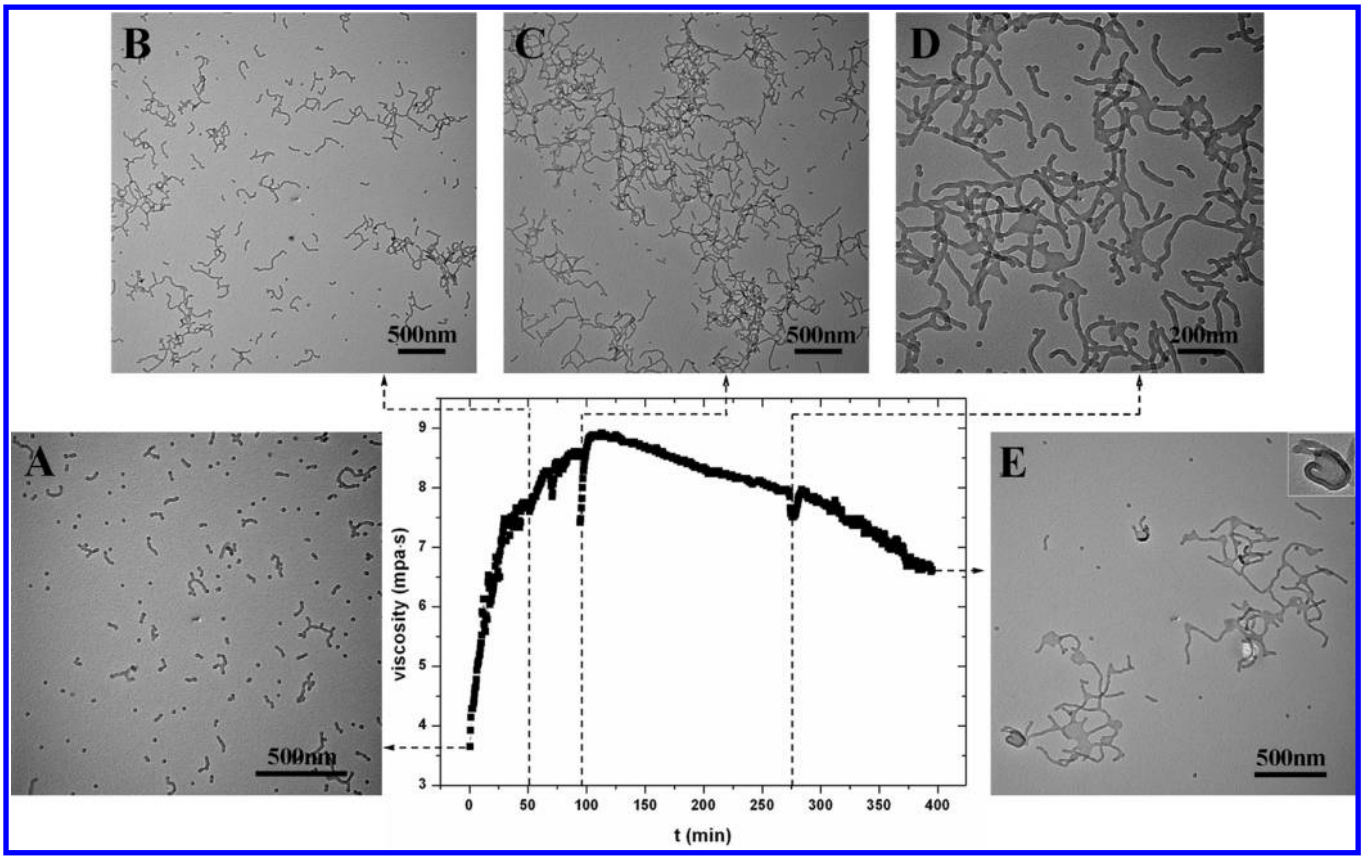

Figure 4. Viscosity as a function of the shear time after adding 30 μL (3.5 mg/mL) of $CaCl_2$ solution into the pre-prepared PS_{144}-*b*-PAA_{22} spherical micelle solution (500 μL). The shear rate is 75 s^{-1}. Several TEM images at different times are given to show the morphological transition pathway: snapshot A, 0 min; snapshot B, 50 min; snapshot C, 94 min; snapshot D, 273 min; and snapshot E, 395 min.

the current study, the solubility parameter of the PS chain (16.6−20.2 $MPa^{1/2}$) is closer to dioxane (20.5 $MPa^{1/2}$) than DMF (24.8 $MPa^{1/2}$). Moreover, the polarity of dioxane (dielectric constant of 2.2) is much lower than that of DMF (dielectric constant of 38.2). This implies that the stretching degree of PS is higher and the repulsion among the PAA corona is lower when dioxane is used as the common solvent. In other words, PS_{144}-*b*-PAA_{50} spherical micelles (in dioxane) are easier to transform to cylindrical micelles and then to vesicles than that of PS_{144}-*b*-PAA_{22} spherical micelles (in DMF), as shown in Figures 1 and 3.

3.2. Online Rheological Investigation on the Morphological Transition Induced by $CaCl_2$. In the prepared PS_{144}-*b*-PAA_{22} spherical micelles (see Figure S1a of the Supporting Information), there are repulsive interactions between the corona-forming PAA chains because of the ionization of PAA blocks. It has been reported that there is a strong binding of Ca^{2+} to the carboxylate group of the PAA block, leading to a decrease of repulsive interactions between PAA blocks.[33] Therefore, the micellar structure can also be tuned by introducing $CaCl_2$. In Figure 4, we show the viscosity of the aqueous solution as a function of the shear time after adding 30 μL (3.5 mg/mL) of $CaCl_2$ solution into the prepared PS_{144}-*b*-PAA_{22} spherical micelle solution (500 μL). Similar to the viscosity−time curve induced by HCl (Figure 1), the viscosity increases rapidly at first and then decreases slowly. TEM images show that the short cylinders (snapshot A) gradually grow into long and entangled cylinders (snapshot C). As a result, the viscosity of the micelle solution is increased. Thereafter, some lamellae appear at the entanglement point of the cylinders (snapshot D). Finally, some lamellae are bending into vesicles, as shown in the snapshot E. Because of the breakup of the entangled structure, the viscosity is correspondingly declined. In Figure S5 of the Supporting Information, we also show the viscosity curve obtained without interrupting the measurement and the TEM images of the morphologies before and after shear to confirm that the loss of a trace amount of solution will not influence the rheological measurement.

After 30 μL of $CaCl_2$ solution is added to the initial prepared PS_{144}-*b*-PAA_{50} spherical micelle solution (500 μL), its viscosity drops rapidly at first (20 min) and then shows a slight decrease with further increasing the shear time, as shown in Figure 5. From the inserted TEM images, it is found that the morphology has already transitioned into lamellae and cylinders before shearing (snapshot A). These lamellae and cylinders turn to the aggregates piled up by many spheres (snapshot B), and then the aggregates disperse into independent spheres or a short cylinder gradually (snapshots C and D). The viscosity curve obtained without interrupting and the TEM images of the morphologies before and after shear are given in Figure S6 of the Supporting Information.

3.3. Influence of the Ion Concentration on Micellar Transitions. In this section, we examine the difference in the viscosities of the micellar transitions induced by adding different concentrations of H^+ or Ca^{2+} into PS_{144}-*b*-PAA_{22} solution. In panels a and b of Figure 6, we present the viscosity−time curves for the morphological transitions at different HCl concentrations and different $CaCl_2$ concentrations, respectively. Moreover, we also present the viscosity curves for the blank sample (without adding ion). Clearly, the

dx.doi.org/10.1021/la503835u | *Langmuir* 2014, 30, 15392−15399

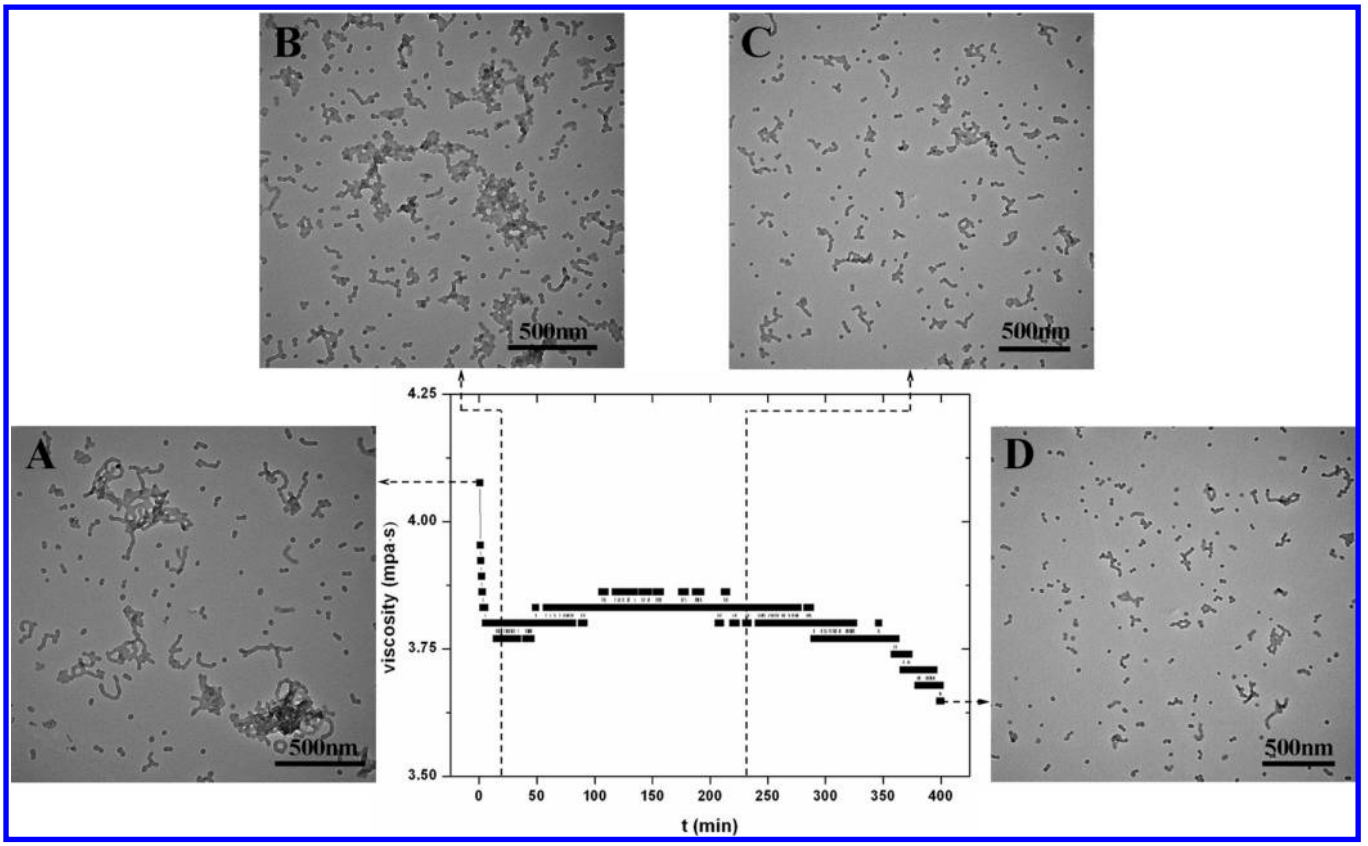

Figure 5. Viscosity as a function of the shear time after adding 30 μL (10 mg/mL) of $CaCl_2$ solution into the pre-prepared PS_{144}-*b*-PAA_{50} spherical micelle solution (500 μL). The shear rate is 75 s^{-1}. Several TEM images at different times are given to show the morphological transition pathway: snapshot A, 0 min; snapshot B, 20 min; snapshot C, 230 min; and snapshot D, 400 min.

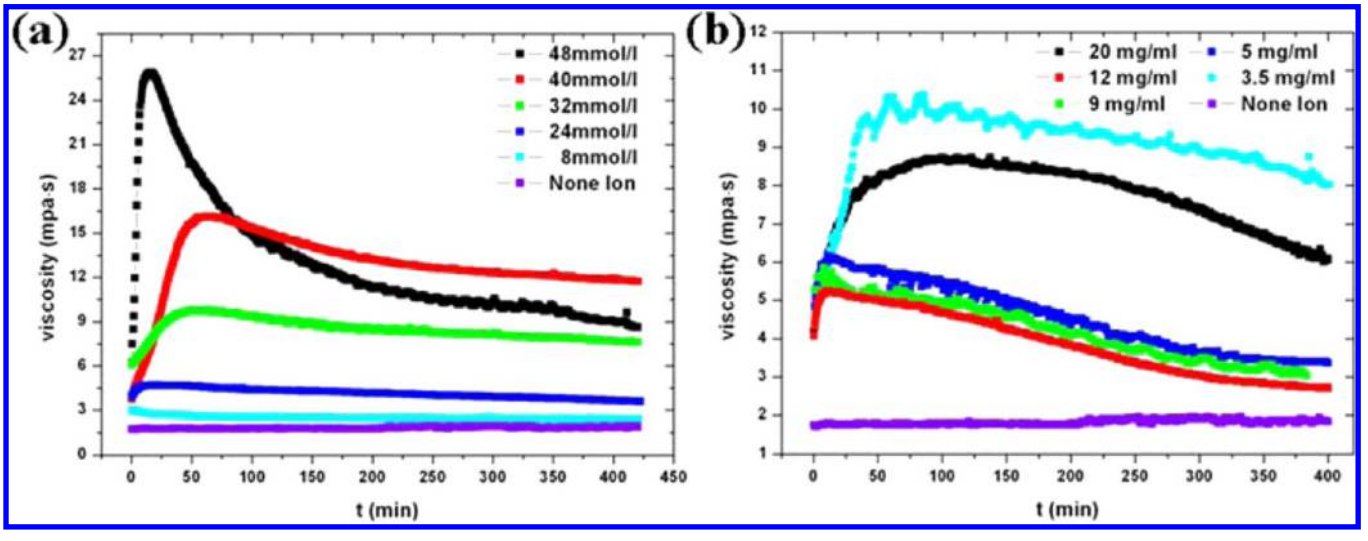

Figure 6. Comparison of the viscosity−time curves after adding different concentrations of ions into PS_{144}-*b*-PAA_{22} spherical micelle solution: (a) adding different concentrations of HCl solution and (b) adding different concentrations of $CaCl_2$ solution.

viscosity for the blank sample remains almost unchanged after shearing for 420 min, indicating that no morphological transition is happening when ions are absent. From Figure 6a, when the concentration of HCl solution is 8 mmol/L, we can see that the viscosity curve is similar to the curve of the solution without adding ion. At this concentration, the morphology remains spherical micelle (see Figure S7 of the Supporting Information), which implies that the morphological transition cannot be induced at a relatively low H^+ concentration. With further increasing of the concentration of H^+, an obvious peak of viscosity is observed. Moreover, the peak value is increased as the H^+ content increased, indicating that more and more long and entangled cylinders are formed during the morphological transition. In Figure 6b, it can be seen that the peak value of the viscosity is decreased at first when the $CaCl_2$ concentration is increased from 3.5 to 12 mg/mL. When the $CaCl_2$ concentration is further increased to 20 mg/mL, however, the peak value of the viscosity is increased. This is

dx.doi.org/10.1021/la503835u | *Langmuir* 2014, 30, 15392−15399

because that the morphological transitions are different at low and high $CaCl_2$ concentrations, which are confirmed by TEM images. When the $CaCl_2$ concentration is in the range of 3.5−12 mg/mL, more and more vesicles are obtained with the increase of the $CaCl_2$ concentration (see Figure 4e and Figure S8a of the Supporting Information). Therefore, the viscosity is decreased as the $CaCl_2$ concentration is increased from 3.5 to 12 mg/mL. However, more long and entangled cylinders are observed when the $CaCl_2$ concentration is further increased to 20 mg/mL (see Figure S8b of the Supporting Information), which makes the viscosity increase again. Figure 6b shows that introducing Ca^{2+} into the PS_{144}-*b*-PAA_{22} spherical micellar solution will cause a sphere−cylinder−vesicle transition. However, a very high concentration of Ca^{2+} will hinder the transformation of cylinder to vesicle, which makes the micellar structure stop at cylinder.

4. CONCLUSION

In the current study, we apply the rheological method to online study the ion-induced micellar transition by the time dependence of the viscosity of the solution under shearing. After ion solution, i.e., HCl or $CaCl_2$ solution, is added to the PS_{144}-*b*-PAA_{22} spherical micelle solution, the spherical micelles will transform into other micelles because of the decrease of repulsive interactions of corona-forming PAA chains. The ion-induced morphological transition can be online-monitored by the time dependence viscosity. It is observed that the viscosity is increased when the spheres transform into long and entangled cylinders. However, when the micelles are further transitioned into lamellae or vesicles, the viscosity is correspondingly declined. When HCl or $CaCl_2$ is added to the prepared spherical micelle solution formed by PS_{144}-*b*-PAA_{50}, the morphologies transform from cylinder aggregates or lamellae to vesicles or spheres, corresponding to a gradual decline in viscosity. The current study shows that the rheological method can be a real-time method for the investigation of micellization and micellar transition of block copolymers in dilute solution.

■ ASSOCIATED CONTENT

Supporting Information

Additional TEM, SEM, and AFM images and viscosity−time curves without interrupting the rheological measurement (Figures S1−S8). This material is available free of charge via the Internet at http://pubs.acs.org.

■ AUTHOR INFORMATION

Corresponding Authors

*E-mail: ytzhu@ciac.ac.cn.
*E-mail: wjiang@ciac.ac.cn.

Notes

The authors declare no competing financial interest.

■ ACKNOWLEDGMENTS

This work was financially supported by the National Natural Science Foundation of China for Youth Science Funds (21104083), the General Program (51373172), the Major Program (51433009), the Scientific Development Program of Jilin Province (201201007), and the Open Project of State Key Laboratory of Supramolecular Structure and Materials (sklssm201411).

■ REFERENCES

(1) Savić, R.; Luo, L.; Eisenberg, A.; Maysinger, D. Micellar nanocontainers distribute to defined cytoplasmic organelles. *Science* **2003**, *300*, 615−618.

(2) Allen, C.; Maysinger, D.; Eisenberg, A. Nano-engineering block copolymer aggregates for drug delivery. *Colloids Surf., B* **1999**, *16*, 3−27.

(3) Bronich, T. K.; Vinogradov, S. V.; Kabanov, A. V. Interaction of nanosized copolymer networks with oppositely charged amphiphilic molecules. *Nano Lett.* **2001**, *1*, 535−540.

(4) Lodge, T. P.; Rasdal, A.; Li, Z. B.; Hillmyer, M. A. Simultaneous, segregated storage of two agents in a multicompartment micelle. *J. Am. Chem. Soc.* **2005**, *127*, 17608−17609.

(5) Wang, G. C.; Henselwood, F.; Liu, G. J. Water-soluble poly(2-cinnamoylethyl methacrylate)-*block*-poly(acrylic acid) nanospheres as traps for perylene. *Langmuir* **1998**, *14*, 1554−1559.

(6) Henselwood, F.; Wang, G. C.; Liu, G. J. Removal of perylene from water using block copolymer nanospheres or micelles. *J. Appl. Polym. Sci.* **1998**, *70*, 397−408.

(7) Yaroslavov, A. A.; Melik-Nubarov, N. S.; Menger, F. M. Polymer-induced flip-flop in biomembranes. *Acc. Chem. Res.* **2006**, *39*, 702−710.

(8) Zhang, L. F.; Eisenberg, A. Multiple morphologies of "crew-cut" aggregates of polystyrene-*b*-poly(acrylic acid) block copolymers. *Science* **1995**, *268*, 1728−1731.

(9) Won, Y. Y.; Davis, H. T.; Bates, F. S. Giant wormlike rubber micelles. *Science* **1999**, *283*, 960−963.

(10) Pochan, D. J.; Chen, Z. Y.; Cui, H. G.; Hales, K.; Qi, K.; Wooley, K. L. Toroidal triblock copolymer assemblies. *Science* **2004**, *306*, 94−97.

(11) Zhu, J. T.; Liao, Y. G.; Jiang, W. Ring-shaped morphology of "crew-cut" aggregates from ABA amphiphilic triblock copolymer in a dilute solution. *Langmuir* **2004**, *20*, 3809−3812.

(12) Discher, D. E.; Eisenberg, A. Polymer vesicles. *Science* **2002**, *297*, 967−973.

(13) Han, Y.; Yu, H.; Du, H.; Jiang, W. Effect of selective solvent addition rate on the pathways for spontaneous vesicle formation of ABA amphiphilic triblock copolymers. *J. Am. Chem. Soc.* **2010**, *132*, 1144−1150.

(14) Zhang, L.; Eisenberg, A. Morphogenic effect of added ions on crew-cut aggregates of polystyrene-*b*-poly(acrylic acid) block copolymers in solutions. *Macromolecules* **1996**, *29*, 8805−8815.

(15) Chen, L.; Shen, H. W.; Eisenberg, A. Kinetics and mechanism of the rod-to-vesicle transition of block copolymer aggregates in dilute solution. *J. Phys. Chem. B* **1999**, *103*, 9488−9497.

(16) Lim Soo, P.; Eisenberg, A. Preparation of block copolymer vesicles in solution. *J. Polym. Sci., Part B: Polym. Phys.* **2004**, *42*, 923−938.

(17) Bhargava, P.; Tu, Y.; Zheng, J. X.; Xiong, H.; Quirk, R. P.; Cheng, S. Z. D. Temperature-induced reversible morphological changes of polystyrene-*block*-poly(ethylene oxide) micelles in solution. *J. Am. Chem. Soc.* **2007**, *129*, 1113−1121.

(18) Yu, H.; Jiang, W. Effect of shear flow on the formation of ring-shaped ABA amphiphilic triblock copolymer micelles. *Macromolecules* **2009**, *42*, 3399−3404.

(19) Davies, T. S.; Ketner, A. M.; Raghavan, S. R. Self-assembly of surfactant vesicles that transform into viscoelastic wormlike micelles upon heating. *J. Am. Chem. Soc.* **2006**, *128*, 6669−6675.

(20) Badiger, M. V.; Rajamohanan, P. R.; Suryavanshi, P. M.; Ganapathy, S.; Mashelkar, R. A. In situ rheo-NMR investigations of shear-dependent ^1H spin relaxation in polymer solutions. *Macromolecules* **2001**, *35*, 126−134.

(21) da Silva, M. A.; Weinzaepfel, E.; Afifi, H.; Eriksson, J.; Grillo, I.; Valero, M.; Dreiss, C. A. Tuning the viscoelasticity of nonionic wormlike micelles with β-cyclodextrin derivatives: A highly discriminative process. *Langmuir* **2013**, *29*, 7697−7708.

(22) Oda, R.; Bourdieu, L.; Schmutz, M. Micelle to vesicle transition induced by cosurfactant: Rheological study and direct observations. *J. Phys. Chem. B* **1997**, *101*, 5913−5916.

(23) Hassan, P. A.; Valaulikar, B. S.; Manohar, C.; Kern, F.; Bourdieu, L.; Candau, S. J. Vesicle to micelle transition: Rheological investigations. *Langmuir* **1996**, *12*, 4350−4357.
(24) Yoshida, T.; Taribagil, R.; Hillmyer, M. A.; Lodge, T. P. Viscoelastic synergy in aqueous mixtures of wormlike micelles and model amphiphilic triblock copolymers. *Macromolecules* **2007**, *40*, 1615−1623.
(25) Eghbali, E.; Colombani, O.; Drechsler, M.; Müller, A. H. E.; Hoffmann, H. Rheology and phase behavior of poly(*n*-butyl acrylate)-*block*-poly(acrylic acid) in aqueous solution. *Langmuir* **2006**, *22*, 4766−4776.
(26) Helgeson, M. E.; Hodgdon, T. K.; Kaler, E. W.; Wagner, N. J.; Vethamuthu, M.; Ananthapadmanabhan, K. P. Formation and rheology of viscoelastic "double networks" in wormlike micelle−nanoparticle mixtures. *Langmuir* **2010**, *26*, 8049−8060.
(27) Shrestha, R. G.; Sakai, K.; Sakai, H.; Abe, M. Rheological properties of polyoxyethylene cholesteryl ether wormlike micelles in aqueous system. *J. Phys. Chem. B* **2011**, *115*, 2937−2946.
(28) Prud'homme, R. K.; Wu, G.; Schneider, D. K. Structure and rheology studies of poly(oxyethylene−oxypropylene−oxyethylene) aqueous solution. *Langmuir* **1996**, *12*, 4651−4659.
(29) Sreejith, L.; Parathakkat, S.; Nair, S. M.; Kumar, S.; Varma, G.; Hassan, P. A.; Talmon, Y. Octanol-triggered self-assemblies of the CTAB/KBr system: A microstructural study. *J. Phys. Chem. B* **2010**, *115*, 464−470.
(30) Watanabe, H.; Matsumiya, Y. Rheology of diblock copolymer micellar dispersions having soft cores. *Macromolecules* **2005**, *38*, 3808−3819.
(31) Morita, C.; Imura, Y.; Ogawa, T.; Kurata, H.; Kawai, T. Thermal-sensitive viscosity transition of elongated micelles induced by breaking intermolecular hydrogen bonding of amide groups. *Langmuir* **2013**, *29*, 5450−5456.
(32) Zhang, L. F.; Yu, K.; Eisenberg, A. Ion-induced morphological changes in "crew-cut" aggregates of amphiphilic block copolymers. *Science* **1996**, *272*, 1777−1779.
(33) Zhang, L. F.; Eisenberg, A. Formation of crew-cut aggregates of various morphologies from amphiphilic block copolymers in solution. *Polym. Adv. Technol.* **1998**, *9*, 677−699.
(34) Liu, F. T.; Eisenberg, A. Preparation and pH triggered inversion of vesicles from poly(acrylic acid)-*block*-polystyrene-*block*-poly(4-vinyl pyridine). *J. Am. Chem. Soc.* **2003**, *125*, 15059−15064.
(35) Shen, H.; Zhang, L.; Eisenberg, A. Multiple pH-induced morphological changes in aggregates of polystyrene-*block*-poly(4-vinylpyridine) in DMF/H_2O mixtures. *J. Am. Chem. Soc.* **1999**, *121*, 2728−2740.
(36) Zhang, L. F.; Eisenberg, A. Crew-cut aggregates from self-assembly of blends of polystyrene-*b*-poly(acrylic acid) block copolymers and homopolystyrene in solution. *J. Polym. Sci., Part B: Polym. Phys.* **1999**, *37*, 1469−1484.
(37) Liu, X.; Wu, J.; Kim, J.-S.; Eisenberg, A. Self-assembly of mixtures of block copolymers of poly(styrene-*b*-acrylic acid) with random copolymers of poly(styrene-*co*-methacrylic acid). *Langmuir* **2006**, *22*, 419−424.
(38) Lei, L. Morphology of core-shell-corona aqueous micelles: II. Addition of core-forming homopolymer. *Polymer* **2004**, *45*, 4375−4381.
(39) Burke, S. E.; Eisenberg, A. Effect of sodium dodecyl sulfate on the morphology of polystyrene-*b*-poly(acrylic acid) aggregates in dioxane−water mixtures. *Langmuir* **2001**, *17*, 8341−8347.
(40) Jacquin, M.; Muller, P.; Cottet, H.; Crooks, R.; Théodoly, O. Controlling the melting of kinetically frozen poly(butyl acrylate-*b*-acrylic acid) micelles via addition of surfactant. *Langmuir* **2007**, *23*, 9939−9948.
(41) Zhu, J.; Ferrer, N.; Hayward, R. C. Tuning the assembly of amphiphilic block copolymers through instabilities of solvent/water interfaces in the presence of aqueous surfactants. *Soft Matter* **2009**, *5*, 2471−2478.
(42) Gao, L.; Shi, L.; Zhang, W.; An, Y.; Liu, Z.; Li, G.; Meng, Q. Polymerization of spherical poly(styrene-*b*-4-vinylpyridine) vesicles to giant tubes. *Macromolecules* **2005**, *38*, 4548−4550.
(43) Wang, Z.; Jiang, W. Temperature-induced reversible transformation between toroidal and cylindrical assemblies under shear flow. *Soft Matter* **2010**, *6*, 3743−3746.
(44) Wang, L.; Yu, X.; Yang, S.; Zheng, J. X.; Van Horn, R. M.; Zhang, W.-B.; Xu, J.; Cheng, S. Z. D. Polystyrene-*block*-poly(ethylene oxide) reverse micelles and their temperature-driven morphological transitions in organic solvents. *Macromolecules* **2012**, *45*, 3634−3638.
(45) *Polymer Handbook*, 4th ed.; Brandrup, J. I., Edmund, H., Grulke, E. A., Abe, A., Bloch, D. R., Eds.; John Wiley & Sons: Hoboken, NJ, 1998.
(46) Yu, Y.; Zhang, L.; Eisenberg, A. Morphogenic effect of solvent on crew-cut aggregates of amphiphilic diblock copolymers. *Macromolecules* **1998**, *31*, 1144−1154.